Experimental, analytical and numerical assessment of the bond-slip behaviour in concrete-filled-FRP tubes

Ahmed Mohamed Ali, Lamine Dieng, Radhouane Masmoudi

Version of Record: https://www.sciencedirect.com/science/article/pii/S0141029620338554
Manuscript_306b23041558fb44cfd12b925b97dedc

EXPERIMENTAL, ANALYTICAL AND NUMERICAL ASSESSMENT OF THE BOND -SLIP BEHAVIOUR IN CONCRETE-FILLED-FRP TUBES

Ali, Ahmed Mohamed[a], Lamine Dieng[b,*], Masmoudi, Radhouane[a]

[a] *Professor, Department of Civil Engineering, University of Sherbrooke, Sherbrooke, QC, Canada, J1K 2R1*
[b] *Research Director, Department of Material and Structure, Univ Gustave Eiffel, Campus de Nantes*

Abstract

The interfacial bond between the fiber-reinforced polymers tube (FRP-T) and its concrete core (CC) is necessary to transfer the loads from the FRP-T to the CC. In this study authors present an experimental investigation of the interfacial bond strength between the circular pultruded FRP-Ts (with or without sand-coating) and a CC. It also aims to evaluate the use of sand-coating as a bond enhancer to improve the interfacial bond strength of the concrete filled FRP tube members. Twelve (12) full-scale circular CFFT specimens with 200mm length and 12,7mm wall thickness were tested, with two different diameters (305 mm and 406 mm) and two different inner surface texture (sand-coated or not). The driving force and the slippage between the FRP-T and its CC were captured to plot the interfacial bond-slip relationships for each specimen. The experimental results showed that the measured interfacial bond stress between the pultruded FRP-T and its CC (without sand-coating) was varying from 0.022 MPa to 0.028 MPa then could therefore be neglected. Meanwhile, the interfacial bond strength of the same tube with sand-coating was varying from 0.43 MPa to 1.00 MPa. Consequently, sand-coating as a bond enhancer was proven to significantly improve the interfacial bond strength of the pultruded FRP-T. This paper also presents results from an analytical model and a F.E. simulation model of the interfacial bond-slip behaviour for CFFT members. Coulomb stick-slip friction model is used to characterise the interfacial connection behaviour between the FRP-T and its CC. Experimental, analytical and numerical results are consistent.

Key words: Concrete-Filled FRP Tubes, Bond-slip Model, Sand-coating, Bond-stress, Analytical Modeling, Numerical Modeling

1. INTRODUCTION

Throughout the past twenty years, concrete-filled fiber reinforced polymer (FRP) tubes (CFFTs) members have been introduced as a structurally efficient alternative to supplant conventional steel-reinforced concrete elements [1], [2]. The FRP tube (FRP-T) serves as formwork and by comparing it to the steel formwork, it considers as a lightweight form-work. Also, because of higher axial and flexural capacities of

*Corresponding author
Email addresses: Ahmed.Ali3@usherbrooke.ca (Ali, Ahmed Mohamed), lamine.dieng@univ-eiffel.fr (Lamine Dieng), Radhouane.Masmoudi@usherbrooke.ca (Masmoudi, Radhouane)

concrete-filled FRP tubes (CFFT), compared to conventional reinforced concrete columns/beams, we can use smaller sections, which means lighter CFFT's structures Concrete filled FRP tubes (CFFTs) have superior resistance against severe environmental conditions, where the FRP-T covers the concrete. So, the concrete core and the internal steel reinforcement will be protected against the exterior deterioration effects. Due to these advantages, CFFTs members have been employed in several structural applications namely; marine constructions, bridges, poles, and over-head sign structures. CFFT members have demonstrated respectable advantages such as permanent lightweight formwork, providing external non-corrosive reinforcement, and confining the CC [3]. These advantages reinforce their durability in the harsh environmental conditions. Moreover, the fact that the CC is confined increases strength, stiffness, and ductility of such members. The improvement of interfacial bonding actually increases the stiffness of concrete-filled-FRP much more than the strength. Notwithstanding that numerous studies [[4]–[5]] have been operated to examine the axial and the flexural behavior of CFFT elements, very little attention has been granted to the influence of the interfacial bond stress between the FRP-T and its CC [[3],[6],[7]]. Stress should effectively transfer from the FRP-T to its CC to achieve the structural superiority of the CFFT members. The interfacial bond strength is altering from case to case based on various factors such as the properties the CC, tube thickness, tube diameter ([8]), and texture of the tube interior surface. Fundamentally, the interfacial bond can be created by using either shear connectors (using resin ribs) or the natural bond between the FRP-T and its concrete (in the case of the rough texture of the interior surface of the tube).

Helmi [9] has tested the bond strength between the CC and filament-wound E-Glass/Epoxy FRP (GFRP) tubes. The interior skin of Helmi's tubes had small circumferential ridges of about 0.3 mm projection and spaced at about 9 mm in the longitudinal direction. Helmi's tubes had an exterior diameter of 367 mm and 5.7 mm tube wall thickness. The height of the tubes was 30 mm. The tubes had been filled with concrete of average cylindrical compressive strength 59 MPa. Super plasticizers had been added to the concrete mixture to guarantee a perfect filling of the tubes. Helmi added an expansive agent to the concrete mixture to compensate the shrinkage of concrete after hardening and prevent separation of the CC from the tubes. Helmi concluded that the bond strength between filament-wound GFRP tube and its CC equals 0.63 MPa. Lai [10] tested six push-through CFFT specimens embedded into reinforced concrete (RC) footings under axial compression load. The aim of Lai's study was to determine the interfacial shear strength (bond) between the filament-wound GFRP tube external surface and the footing concrete. Due to the filament-wound fabrication process of the GFRP tubes, the external tube surfaces had an undulating structure in the longitudinal direction. The distance between the ripples was about 25 to 30 mm. The thickness of the ripples was about 0.1 to 0.2 mm. The concrete of the RC footings had a compressive strength of 41 MPa. Based on Lai's experimental results for this GFRP tubes, the ultimate bond strength between the exterior surface of the GFRP tube and the concrete mean value is evaluated equal to 0.75 MPa, while this value can be affected by several parameters such as the surface texture, FRP-T fabrication process , concrete failure modulus, and confining steel reinforcement in the footing. The bond-slip stress of the tested specimens has been divided at

least by 2 when the bond reached the ultimate strength. In Lai's study the RC footing was the surrounding material and the tube had been pushed through the RC footing. Consequently, the interfacial bond strength in the case of the FRP-T surrounding its CC might be different than Lai's tests. Obviously, the interfacial bond between the FRP-T and its CC is the key parameter, to evaluate the full composite action in CFFT members especially those subjected to bending loads [3]. Excessive slip occurs at the interface between the concrete and the FRP-T, due to the lack of the interfacial bond strength. This slip may adversely affect the composite action of the CFFT member. This paper presents experimental results of push-out tests conducted on circular CFFT specimens. The interfacial bond strength between the circular pultruded FRP-T and its concrete core is investigated for two different tube diameters (305 mm and 406 mm). For half of the specimens (6 specimens), the inner surface of the pultruded FRP-Ts has been roughened by sand-coating to increase the interfacial bond between the tube and its CC, while the other half has been left unhandled. Up-to-date, there are no standards or guidelines that have been issued to test or evaluate the interfacial bond strength between the FRP-T and its CC. In previous studies on CFFTs, no numerical or analytical bond-slip models have been presented. Therefore, this paper evaluates the interfacial bond-slip relationship and investigates the contribution of using sand-coating as a bond enhancer to improve the interfacial bond strength in CFFT members. This study is important to fully understand and measure the mechanical behavior of the bond interface between concrete and the FRP Tube. The results will be used to optimize the design of CFFT's structures under flexural or combined flexural/axial loads

2. EXPERIMENTAL SETUP AND PROGRAM

The experimental program is composed of twelve CFFT push-out specimens submitted to push-out test. The push-out test is to apply a vertical load on the top and center of the CC only. The FRP-T is supported vertically on the bottom end. The load is transferred from the CC to the FRP-T by the interfacial bond. The interfacial bond stress can be evaluated as the load divided by the contact surface between the FRP-T and concrete. This section describes the specimen's constituent materials, the specimen's configurations, the experimental test setup, and instrumentations.

2.1. Structural Components Properties

Two components have been used in this experimental program: The first material is the FRP-T while the second one is and the CC. The following points provide the characterization of the reported materials in this research.

2.1.1. FRP Tube

The Tubes used for experimental test are circular pultruded FRP-Ts. The tube manufacturing processes are detailed in [[11] and [12]]. Two different tube sections have been used; 305 mm and 406 mm (S-305 refers to tubes with 305 mm of diameter while S-406 indicates tube with 406 mm of diameter). The thickness of

Tubes ID	D_0 (mm)	t_f (mm)	h (mm)	f_{cl} (MPa)	f_{tl} (MPa)	E_l (GPa)
S-305	305	12.7	200	555	665	36.5
S-406	406	12.7	200	572	711	38

Table 1: FRP Tube Properties

the tube is considered as constant for all specimens and is equal to 12.7 mm. A total of 12 specimens (6 for each category of tubes), were tested under uniaxial tension and compression in order to determine the axial mechanical properties of each type FRP-T following the ASTM D3039/D3039M [13] and ASTM D695 [14], respectively. The geometrical and mechanical characteristics of both tubes are shown in Table 1. D_o , t_f, h, are respectively the tube outer diameter, the tube thickness, the tube height, and f_{cl} , f_{tl} and E_l are respectively the average compressive strength, the average tensile strength, and the elasticity modulus.

2.1.2. Concrete

The filling material for the tubes is prepared from ready-mixed concrete with a theoretical characteristic resistance of 35 MPa (C35/45). The size of the aggregate is between 5-20 mm. Nine cylinders and 6 prisms were prepared on the same day of the test to be used for the characterization of the concrete material. The results obtained after characterization tests on the cylindrical specimens gave a compressive stress at break of 35 MPa ± 2 MPa and the modulus of rupture of prisms was 4.0 MPa ± 0.3 MPa.

2.2. Test Specimens

A total of twelve push-out specimens of two different diameters are tested. These twelve specimens are divided into four groups (S-305, S-305-S, S-406, S-406-S). Each group has three identical specimens. Groups S-305 and S-406 have no sand-coating on their interior surface and have been fabricated from the tubes with outer diameter of 305 mm and 406 mm, respectively. While, groups S-305-S and S-406-S have sand-coating on their interior surface and have been also fabricated with the same tube diameter as groups S-305 and S-406. The fabrication of the specimens starts by cutting the FRP circular tubes to the required length (200 mm). The interior tube surface of two groups was coated with Vinyl ester resin then covered with large-size silica sand particles to provide a rough texture to enhance the interfacial bond. Figure 1 shows a typical schematic for the specimen's details. The bottom end of the tubes has been closed by plastic sheets to avoid the leakage of the concrete water; as shown in figure 2. Afterwards, the FRP-Ts have been filled with concrete.

2.3. Experimental Setup and Instrumentations

Concrete-Filled-FRP tubes are tested in a 60,000-pound Baldwin-Lima-Hamilton Test Machine. Tubes S-305 and S-406 were supported at the bottom on steel tubes with 305 mm and 406 mm external diameter, respectively. The steel tube is supported by three steel stiffeners; as shown in figure 3. The height of the stiffeners is higher than the steel tube by 25 mm to ensure that the FRP-T rested on the steel tube and its

exterior surface is aligned with the steel tube exterior surface. The steel tubes have 6 mm wall thickness which is less than the FRP-Ts wall thickness by 6.7 mm. Therefore, the CC can be driven downward without any obstacles. Vertical axial load (P) was applied by the machine head to the CC This load is resisted by the interfacial bond between the CC and the FRP-T. Two linearly variable displacement transducers (LVDTs) were used to measure the relative slip between the CC and the FRP-T; as shown in figure 3. The load and the LVDTs measurements have been recorded using a data acquisition system with a sampling frequency of 10 Hz.

2.4. Experimental Results

The experimentally recorded load-slip responses for the tests are shown in figure 4. The captured slip value of the right-LVDT was approximately identical with the value of the left-LVDT. Consequently, the average slip value is used to plot all responses in this paper. Generally, all specimens demonstrated the same behavior until the ultimate load was reached. After That, the load dropped to a level of about 35% to 45% of the ultimate load for the specimens without sand-coating. While the recorded load for the specimens with sand-coating decreased gradually with increasing the relative-slip value due to the high friction/adhesion between the sand-coated tube and the CC after the debonding occurred. The ultimate load of the specimens without sand-coating has been captured at a relative-slip value located between 0.3 mm and 1 mm; as shown in figure 4(a) and 4(b). While the ultimate recorded load of the specimens with sand-coating has been observed at a relative-slip value located between 0.28 mm and 1.64 mm; as shown in figure 4(c) and 4(d). Table 2 presents a summary of the experimental results of the tested specimens. Specimen S-406-1 shows an ultimate load two-times higher than the other specimens in the same size. However, its slip value at the ultimate load is approximately in the same range as the other specimens. Therefore, this specimen has been excluded from the analysis.

The interfacial bond stress (τ) is calculated by dividing the vertical load (P) by the contact area (A_C) between the FRP-T and its CC. The contact area is the internal surface area of the FRP-T minus the slipped surface area out the FRP-T; as shown in figure 5; where (δ) is the average relative-slip value corresponding to the vertical load (P). Consequently, the interfacial bond stress at any point during the test equals the vertical load divided by the contact area, as shown in Eq.1. The interfacial bond-slip relationships of the tested specimens are shown in figure 6.

$$\tau = \frac{P}{A_c} = \frac{P}{\pi D_i (h - \delta)} \tag{1}$$

All specimens experience an initial linear curve until the ultimate interfacial bond strength is reached. Gradual drop has been noticed after the bond stress reached the ultimate bond strength. With the excessive slip, the bond stress seems to be constant and equal to respectively 35% to 45% and 40% to 75% on the ultimate bond strength for the specimens without and with sand-coating; respectively. After neglecting the specimen S-406-1, the average interfacial bond strengths for specimens S-305 and S-406 are 30 KPa and 22.5 KPa;

Tube ID	S-305-1	S-305-2	S-305-3	Average	S-406-1*	S-406-2	S-406-3	Average
$P_{max}(N)$	4546	5043	6845	5478	11565	6056	6441	6249
$\delta_{ul}(mm)$	1.01	0.57	0.93	0.84	0.46	0.53	0.31	0.42
$\tau_{max}(KPa)$	25	28	38	30	47	22	23	22.5
Tube ID	S-305-1	S-305-2	S-305-3	Average	S-406-1	S-406-2	S-406-3	Average
$P_{max}(N)$	170780	164764	196482	177342	128125	112732	118181	119679
$\delta_{ul}(mm)$	0.65	0.28	0.94	0.62	1.04	1.64	0.85	1.17
$\tau_{max}(KPa)$	878	840	1000	906	427	439	456	441

* Sepecimen S-406-1 has been excluded from the analysis.

Where ($P_{max}(N)$ is the ultimate load, ($\delta_{ul}(mm)$) is the average slip value corresponding to the ultimate load, and ($\tau_{max}(KPa)$) is the interfacial bond strength between the pultruded FRP tube and its concrete core.

Table 2: Summary of Results

respectively. While, the average interfacial bond strengths for specimens S-305-S and S-406-S are 906 KPa and 441 KPa; respectively.

After the failure of the specimen without sand coating, the CC surface was smooth and no concrete parts stuck to the FRP-T as shown in figure 7(a) and 7(b). For the specimens S-305-S, as shown in figure 8(a) and 8(b), with sand-coating, some parts of the sand-coating layer remained attached to the FRP-T and some parts stuck in the CC. For the specimens S-406-S, the sand coating layer has completely stuck in the CC; as shown in figure 9(a) and 9(b).

3. DISCUSSION

3.1. Contribution of Using Sand-Coating as a Bond Enhancer

Sand-coating increases the interfacial bond strength between the pultruded FRP-T and its CC. Based on the experimental results, sand coating increased considerably the interfacial bond strength by 30 times (from 0.03 to 0.9 MPa) and 20 times (from 0.02 to 0.45 MPa) for the specimens with the outer diameters of 305 mm and 406 mm; respectively. Using sand-coating for the pultruded FRP-Ts achieved interfacial bond strength (0.9 MPa) slightly higher than the strength reported by Helmi [9] (0.63 MPa) for the filament-wound FRP-T with small circumferential ridges of about 0.3 mm projection and spaced at about 9 mm in the longitudinal direction. However, the comparison with Helmi's tubes is not totally correct because there is variation in the concrete properties (the used concrete compressive strength in this paper 35 MPa while Helmi had 59 MPa) and the tube inner diameter (the tube inner diameter in this paper 292.3 mm while Helmi had 355.6 mm). In addition, Helmi used an expansive agent added to the concrete mixture to compensate the shrinkage of concrete after hardening. This comparison might provide a trending about the contribution of using sand-coating and its efficiency. The interfacial bond strength between the pultruded FRP-T and its

CC is very small and can be neglected due to the very smooth texture of the internal surface of such FRP-T. The pultruded FRP-T should not be used in bending application without using any bond-enhancer between the FRP-T and its CC. The shear connectors between the pultruded FRP-T and its CC like resin-ribs could be a method to improve the interfacial bond between the FRP-T and its CC. Using sand coating on the interior surface of the FRP-T could also enhance the interfacial bond between the pultruded FRP-T and its CC.

3.2. Effect of Concrete Core Diameter on the Interfacial Bond Strength

The load force use to push the concrete out of the FRP-T seems to be almost constant for each diameter, then the average bond strength of the tube with a small diameter (S-305 and S-305-S) is higher than the bond strength of the tube with the higher diameter (S-406 and S-406-S). Increasing the interior diameter (then contact surface) of the FRP-T without sand-coating by 36% from 279.6 mm to 380.6 mm decreased the interfacial bond strength by 33% from 0.03 MPa to 0.0225 MPa. While increasing the interior diameter of the FRP-T without sand-coating by 36% from 279.6 mm to 380.6 mm decreased the interfacial bond strength by 51% from 0.9 MPa to 0.44 MPa.

4. ANALYTICAL AND FINITE ELEMENT MODELLING

4.1. Analytical model

Several analytical stress-strain model models for CFFT column was proposed [15]. Some of them has described the bond-slip model between concrete and FRP rebars for internally fiber reinforced concrete members. While up to date, no research has been conducted to present a complete bond-slip model which combining analytical and finite element model for CFFT members. The proposed analytical model consists of evaluating the interface bond-slip behaviour between the FRP-T and its concrete which will be use in the finite element model as the evolution of friction coefficient. It consists of two branches; the ascending branch and the softening branch, as shown in figure 10. The ascending branch of this bond-slip ($S \leq Smax$) relationship is proposed in Eq.2. Where α, β, and γ are empirical parameters which were determined by fitting the analytical relationship with the experimental curve. S is the relative slip between the FRP-T and the CC corresponding to the bond stress. S_{max} is the slip value at the maximum bond stress $\tau_m ax$.

$$\frac{\tau}{\tau_{max}} = \alpha \left[\frac{S}{S_{max}}\right]^3 + \beta \left[\frac{S}{S_{max}}\right]^2 + \gamma \left[\frac{S}{S_{max}}\right] \tag{2}$$

The softening branch of the bond-slip model is governed by Eq.3. where this behavior was mentioned for the first time by Malvar [16] for the bond stress-slip model of FRP rebars. Where a and b are empirical parameters which were determined by fitting of the analytical relationship with the experimental curve.

$$\frac{\tau}{\tau_{max}} = \frac{a\left[\frac{S}{S_{max}}\right] + (b-1)\left[\frac{S}{S_{max}}\right]^2}{1 + (a-2)\left[\frac{S}{S_{max}}\right] + b\left[\frac{S}{S_{max}}\right]^2} \tag{3}$$

Tubes ID	α	β	γ	a	b
S-305	2.6	-5.6	4	1.5	1.4
S-305-S	2.6	-5.6	4	13.5	1.4
S-406	2.2	-4.8	3.6	6	1.2
S-406-S	2.2	-4.8	3.6	16.5	3.5

Table 3: The values of the empirical parameters used in the proposed analytical model

The empirical parameters were determined for each type of specimens in the current study. Table 3 shows the values of these parameters. The analytical results are compared to the experimental results for all specimens, as shown in figure 11 for the ascending branch and figure 12 for the softening branch. It is clear from the figures 11 and 12 that the analytical model and the experimental results are very closed. The proposed analytical model is describing well the interfacial bond-slip relationship for CFFT members.

4.2. Finite Element Model

Using the analytical modelling, a finite element model representing the interfacial bond-slip relationship for CFFT members is proposed in this section. This model is fitted with the experimental results. The aim of this finite element modelling is to evaluate if a classic friction model is able to fit with the experimental results. For this study a Full 3-D model was initially proposed (Fig. 14-a) and then replace by a 3D-axisymmetric model shown in figure 14-b) to reduce the calculation time. The full-scale experimental investigation is modeled using Marc/Mentat finite element tools. This FEM code is distributed by MSC Software [15]. As shown in Fig. 14-b, the axisymmetric model is composed by two contact bodies: FRP body and Concrete body. The two contact bodies are meshed separately with the same elements size. The steel tube which is used to maintain the bottom FRP-T is not represented in this model. It is represented by additional boundary condition. Element type 10 as referenced by the MSC Software library [17] is used for both bodies. The element type 10 is detailed in [18].

The boundary conditions of the model are detailed in Fig. 14-b. A displacement up to 20 mm is applied in one external node which is tied to several nodes of the concrete body. The reaction force appearing at this node corresponds to the application load named P in the analytical model. For the purpose of numerical calculation, displacement along y-axis of the four bottom nodes of the FRP is not allowed. The constitutive behavior of the concrete and the FRP are given in section 2.1.

Four models were analysed, corresponding to two tube diameters (D1 = 305 and D2 = 406) and two surface states (sanded or not-sanded). Model M305 and Model M406 are not sanded in the interface between FRF and concrete; Models M305-S and M406-S are sanded.

The behaviour at the interface between the FRP and the concrete is assumed to be governed by the stick-slip Coulomb's friction law. The friction law is given by

$\|\sigma_t\| < \mu.\sigma_n$ or $\|f_t\| < \mu.f_n$ for perfect adhesive connection,

and

$\|\sigma_t\| = -\mu.\sigma_n \frac{vr}{\|vr\|}$ or $\|f_t\| = \mu.f_n \frac{\Delta ut}{\|\Delta ut\|}$ for gross slip regime.

Where σ_n the normal stress or f_n the normal force is linked to the friction stress σ_t or force f_t by a step function behavior based upon the value of the relative sliding velocity vr or the tangential relative incremental displacement Δut. In this paper two different surfaces need to be characterised. The friction coefficient μ, the normal/adhesion force (f_n) and its evolution need to be identified from the experimental result for each specimen. A simple model is then derived from Coulomb's law to describe phenomena of slip and adhesion. We assume that the friction coefficient could be written for each model by:

$$\mu = \alpha_{mi}.\mu^* \tag{4}$$

and f_{ni} which characterised the adhesion/normal force between the FRP and the concrete depends on the state of the interface and are responsible for the change of the reaction force and the to stress bond interface.

From the analytical results which fit with the experimental mean value of the stress bond interface, one can identify the evolution of μ^* (normalised friction coefficient) for the four cases (see fig. 15). The assumption made here is that the evolution of the bond stress in the interfacial zone is governed by the change of friction coefficient. Then the evolution of μ^* is identified from the analytical equation [[3] & [4]].

Two parameters α_{mi} and f_{ni} need to be identified for each model. They depend on the size of the interface surface (to the diameters) and its state (sanded or not). For the two first models (M305 and M305-S) one fixes first arbitrary α_{mi} as a constant value and then identifies the best value of f_{ni} which is linked to surface state. The rougher the surface is, the more important the adhesion force is. One noticed that the ratio of the two adhesion forces is very close to the ratio of the pick-amplitude ration of the interface mean stress value. As mentioned in the previous section, sand coating increased the interfacial bond strength by 3000 %. The same method is also applied the M406 and M406-S. However, in order to get the size of the contact surface, the parameter α is reduced proportionally to the increase of the surface by:

$$\alpha_{D2} = \alpha_{D1}(1 - \eta) \tag{5}$$

with

$$\eta = \frac{2\|\Delta D|}{D_1 + D_2} \tag{6}$$

With D_1 and D_2 respectively the diameter of the S305 and S406, η is about 28.5. The identified parameters are given in table 4. Figures 16 and 17 show the comparison between the finite element model results and the experimental results in terms of loads and interfacial bond stresses. The proposed FE model seems to be well presenting the interfacial bond-slip relationship for CFFT members.

5. CONCLUSIONS

This paper has experimentally investigated the interfacial bond between the pultruded FRP-T and its CC. The experimental program described in this paper is a part of the ongoing research of the authors on

	M305	M305-S	M406	M406-S
α_{mi}	0.35	0.35	0.25	0.25
$f_{ni}(N)$	0.5	14.25	0.5	10.18

Table 4: Parameters identification of friction law $\|ftmi\| \leq \alpha_{mi}\mu^*.fni$

the effect of the interfacial bond between the pultruded circular FRP-T and its CC on the behavior of the CFFT member and how to improve the composite action between the tube and its CC. This paper has also investigated the contribution of using sand-coating on the interior surface of the FRP-T to enhance the interfacial bond of the CFFT members. Twelve push-out specimens have been tested with two different tube-diameters. The main conclusions of this study are the following:

1. The interfacial bond strength between the studied pultruded FRP-T and its CC are very low (0.022 MPa to 0.03 MPa) and can be neglected due to the smooth texture of the interior surface of the FRP-T.
2. Using sand-coating as a bond enhancer improved the interfacial bond of the CFFT member by 2000% to 3000% in comparison to the specimens without sand-coating.
3. Increasing the FRP-T diameter reduces the interfacial bond between the FRP-T and the CC.
4. Using concrete-filled pultruded FRP-T in structural application subjected to flexural loads should include adequate method to improve the interfacial bond strength as using shear connectors or using sand coating on the interior surface of the FRP-T.
5. An analytical bond-slip model for CFFT member is proposed based on the experimental results.
6. The proposed FEM gives results fitting with the experimental thanks to Coulomb friction model
7. Model parameters identification is derived from the analytical model and parameters depend on to size of the tube.

Acknowledgements

The authors acknowledge the Natural Sciences and Engineering Research Council of Canada (NSERC) for sponsoring this research. The authors also acknowledge the contribution of the Canadian Foundation for Innovation (CFI) for the infrastructure used to conduct these experimental tests. Special thanks to the tube manufacturer (Creative Pultrusions, PA, USA) for providing FRP-Ts, to the technicians Mr. Steven Maceachern and Mr. Sébastien Rioux for the preparation of the Test-Setup.

References

[1] A. Abouzied, R. Masmoudi, Structural performance of new fully and partially concrete-filled rectangular frp-tube beams, Construction and Building Materials 101 (2015) 652 – 660. doi:https://doi.org/10.1016/j.conbuildmat.2015.10.060.
URL http://www.sciencedirect.com/science/article/pii/S0950061815304815

[2] M. Lai, Y. Liang, Q. Wang, F. Ren, M. Chen, J. Ho, A stress-path dependent stress-strain model for frp-confined concrete, Engineering Structures 203 (2020) 109824. doi:https://doi.org/10.1016/j.engstruct.2019.109824.
URL http://www.sciencedirect.com/science/article/pii/S0141029619323466

[3] A. M. Ali, D. Robillard, R. Masmoudi, I. M. Khan, Experimental investigation of bond and tube thickness effect on the flexural behavior of concrete-filled fpr tube under lateral cyclic loading, Journal of King Saud University - Engineering Sciences 31 (1) (2019) 32 – 41. doi:https://doi.org/10.1016/j.jksues.2017.09.005.
URL http://www.sciencedirect.com/science/article/pii/S101836391730123X

[4] H. M. Mohamed, R. Masmoudi, Flexural strength and behavior of steel and frp-reinforced concrete-filled frp tube beams, Engineering Structures 32 (11) (2010) 3789 – 3800. doi:https://doi.org/10.1016/j.engstruct.2010.08.023.
URL http://www.sciencedirect.com/science/article/pii/S0141029610003123

[5] H. M. Mohamed, R. Masmoudi., Axial load capacity of concrete-filled frp tube columns: Experimental versus theoretical predictions., J Compos Constr.

[6] A. M. Ali, R. Masmoudi, Flexural strength and behavior of circular sand-coated concrete-filled frp tubes under cyclic load., ACI Special Publication 327 (2018) 1–54.

[7] A. M. Ali, R. Masmoudi, I. M. Khan, Effect of sand-coating bond performance on the flexural capacity of circular concrete-filled frp tubes, in: 6th Int Conf Eng Mech Mater, 2017.

[8] C. W. Roeder, B. Cameron, C. B. Brown, Composite action in concrete filled tubes, Journal of Structural Engineering 125 (5). doi:https://doi.org/10.1061/(ASCE)0733-9445(1999)125:5(477).

[9] K. Helmi, The effects of driving forces and reversed bending fatigue of concrete-filled frp circular tubes for piles and other applications., Thèse, The University of Manitoba (2007).

[10] Y. C. Lai, Moment connections of concrete-filled fibre reinforced polymer tubes to reinforced concrete footings., Thèse, Queen's University Kingston, Ontario, Canada, (2010).

[11] C. P. Inc., Creative pultrusions inc: Product brochure superpiletm fiberglass reinforced polymer (frp) pipe piles, Alum Bank,PA (2015).

[12] A. M. Ali, R. Masmoudi, Composite action assessment of concrete-filled frp tubes subjected to flexural cyclic load, Engineering Structures 203 (2020) 109889. doi:https://doi.org/10.1016/j.engstruct.2019.109889.
URL http://www.sciencedirect.com/science/article/pii/S014102961930879X

[13] ASTM D3039 standard test method for tensile properties of polymer matrix composite materials (2014).

[14] ASTM D695 standard test method for compressive properties of rigid plastics: (2010).

[15] J. Ho, X. Ou, M. Chen, Q. Wang, M. Lai, A path dependent constitutive model for cfft column, Engineering Structures 210 (2020) 110367. doi:https://doi.org/10.1016/j.engstruct.2020.110367.
URL http://www.sciencedirect.com/science/article/pii/S0141029619348138

[16] L. J. Malvar, Bond stress-slip characteristics of frp rebars., Tech. Rep. TR-2013-SHR, Naval Facilities Engineering Service Center, Port Hueneme,CA (February 1994).

[17] M. Software, Marc 2018.1 Volume A : Theory and User Information., 2018th Edition, MSC Software, 81829 Munich, Germany, 2018.

[18] L. Dieng, P. Marchand, F. Gomes, C. Tessier, F. Toutlemonde, Use of uhpfrc overlay to reduce stresses in orthotropic steel decks, Journal of Constructional Steel Research 89 (2013) 30 – 41. doi:https://doi.org/10.1016/j.jcsr.2013.06.006.
URL http://www.sciencedirect.com/science/article/pii/S0143974X13001727

6. figure

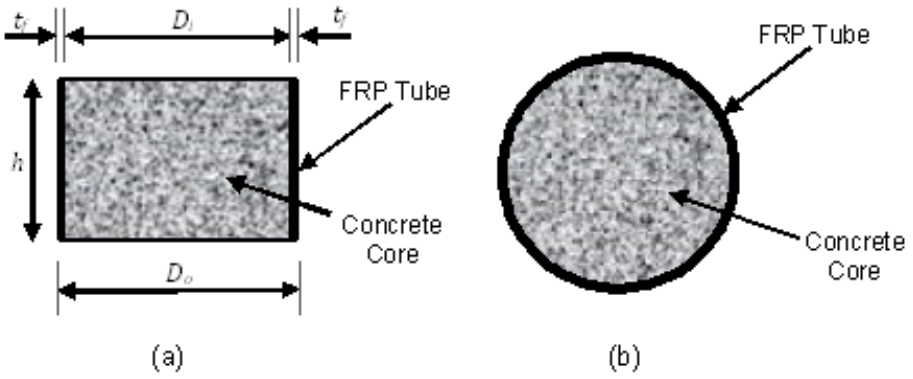

Figure 1: Schematic showing specimen details: (a) Cross-sectional elevation, (b) Cross-section view

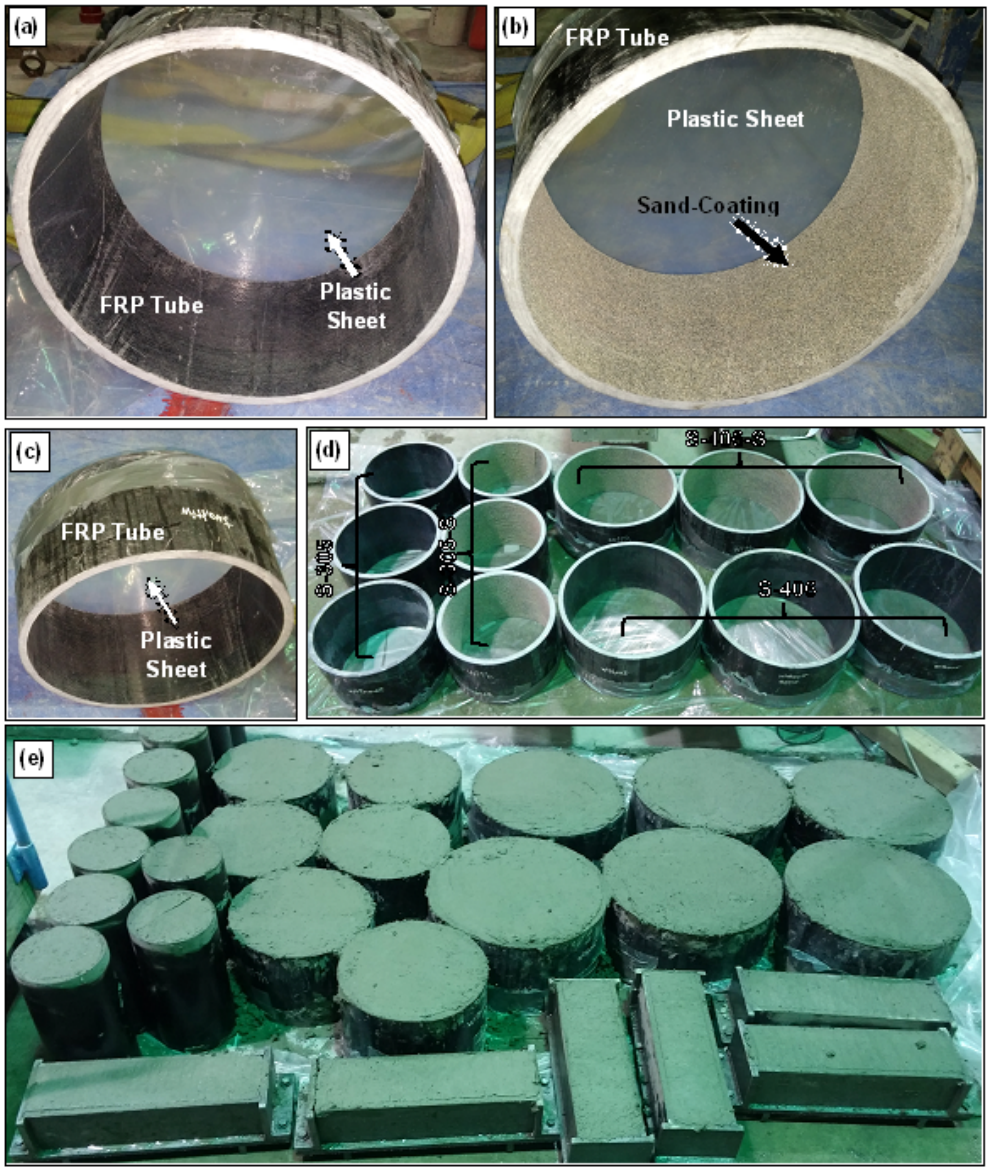

Figure 2: Preparation of specimens: (a) Specimen without sand-coating, (b) Specimen with sand-coating, (c) Closing of the bottom end of the specimen, (d) All specimens before concrete casting, (e) Specimens before casting of concrete

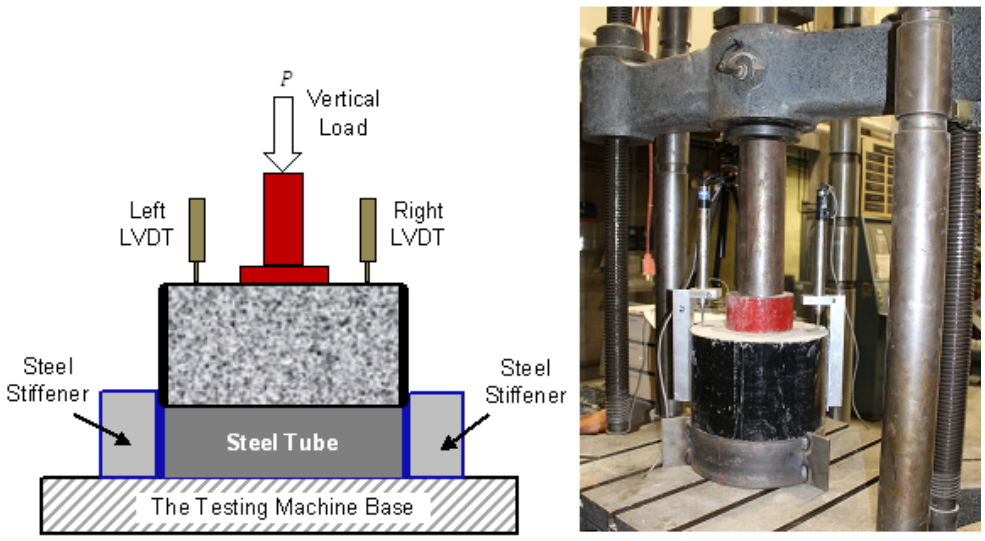

Figure 3: Typical Specimen and Method of Load Application in a 60,000-pound Baldwin-Lima-Hamilton Test Machine

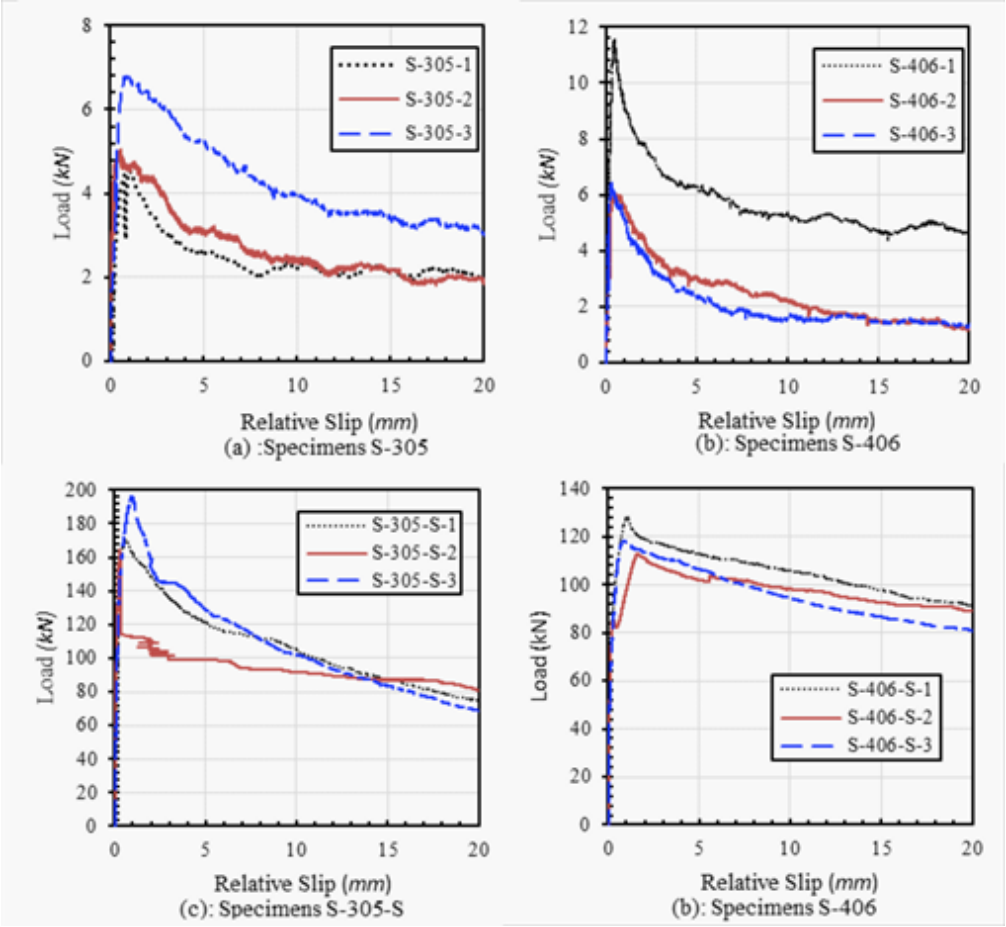

Figure 4: Load-relative slip relationships for the tested specimens

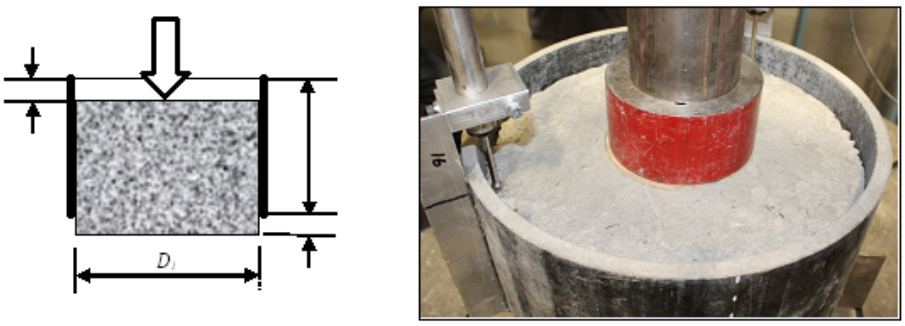

Figure 5: Schematic showing the slipping of the concrete core out the FRP-T

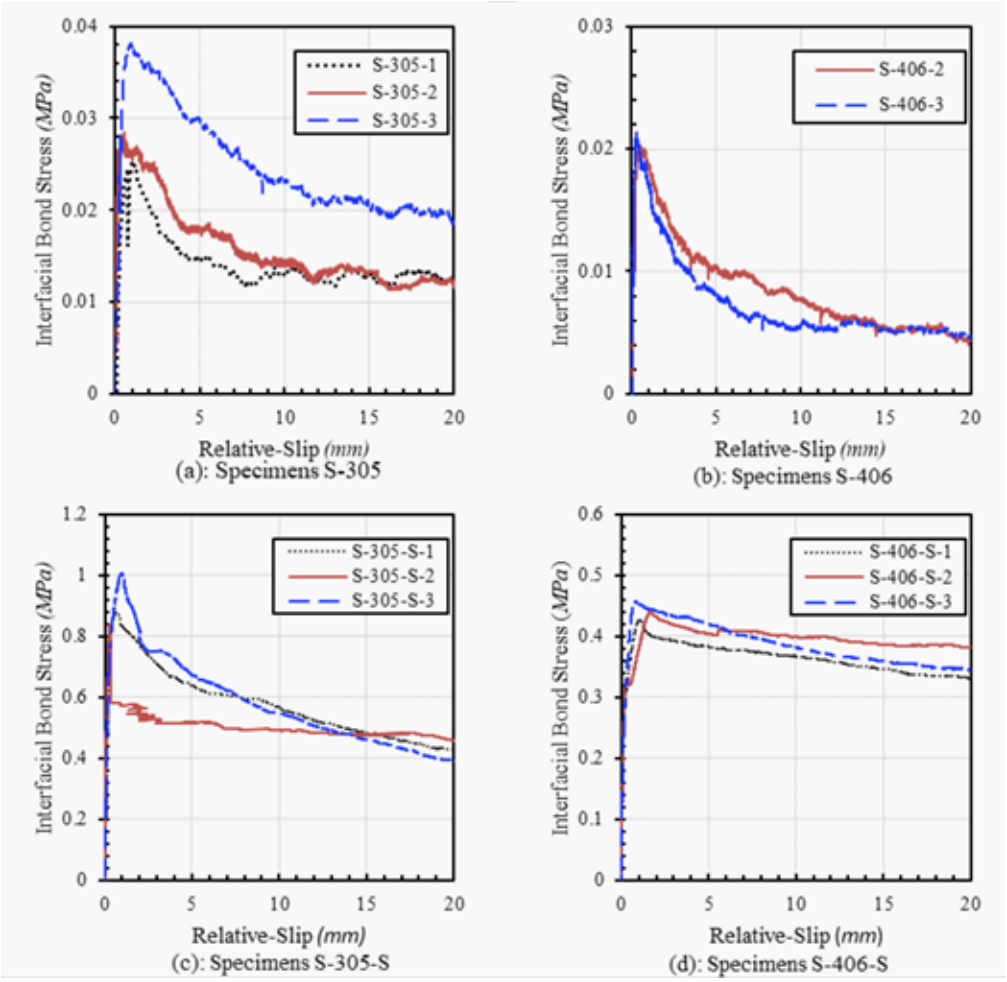

Figure 6: Interfacial bond-relative slip relationships for the tested specimens.

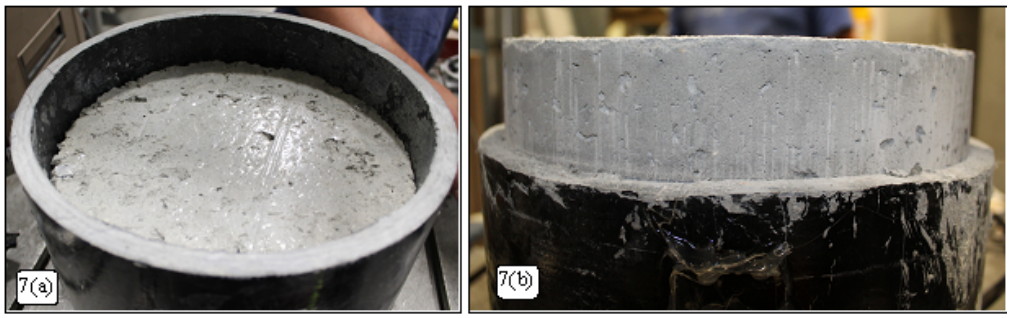

Figure 7: Specimens S-305 and S-406 after failure: (a) The smooth interior surface of the FRP tube, (b) The smooth surface of the concrete core.

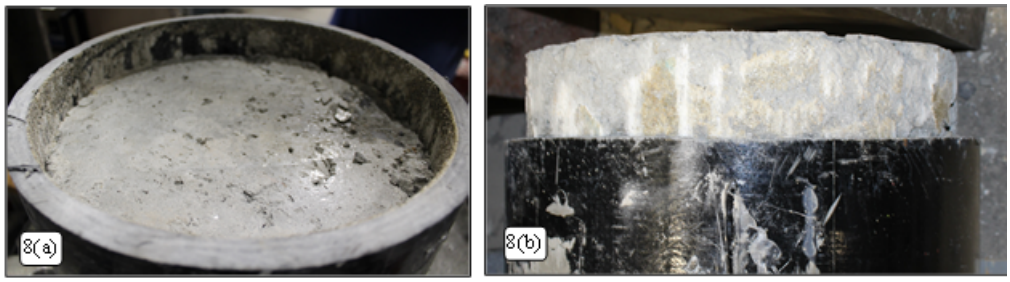

Figure 8: Specimens S-305-S after failure: (a) Some parts of the sand-coating layer attached the FRP tube, (b) The remaining parts of the sand-coating layer have stuck in the concrete core.

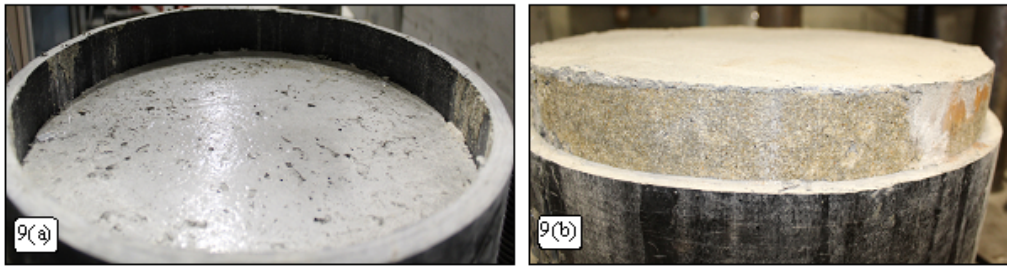

Figure 9: Specimens S-304-S after failure: (a) The interior surface FRP-T approximately smooth, (b) The sand-coating layer has completely stuck in the CC.

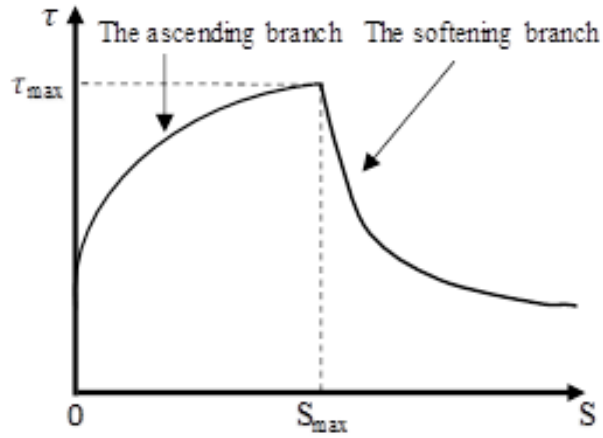

Figure 10: The proposed analytical bond-slip model for CFFT members.

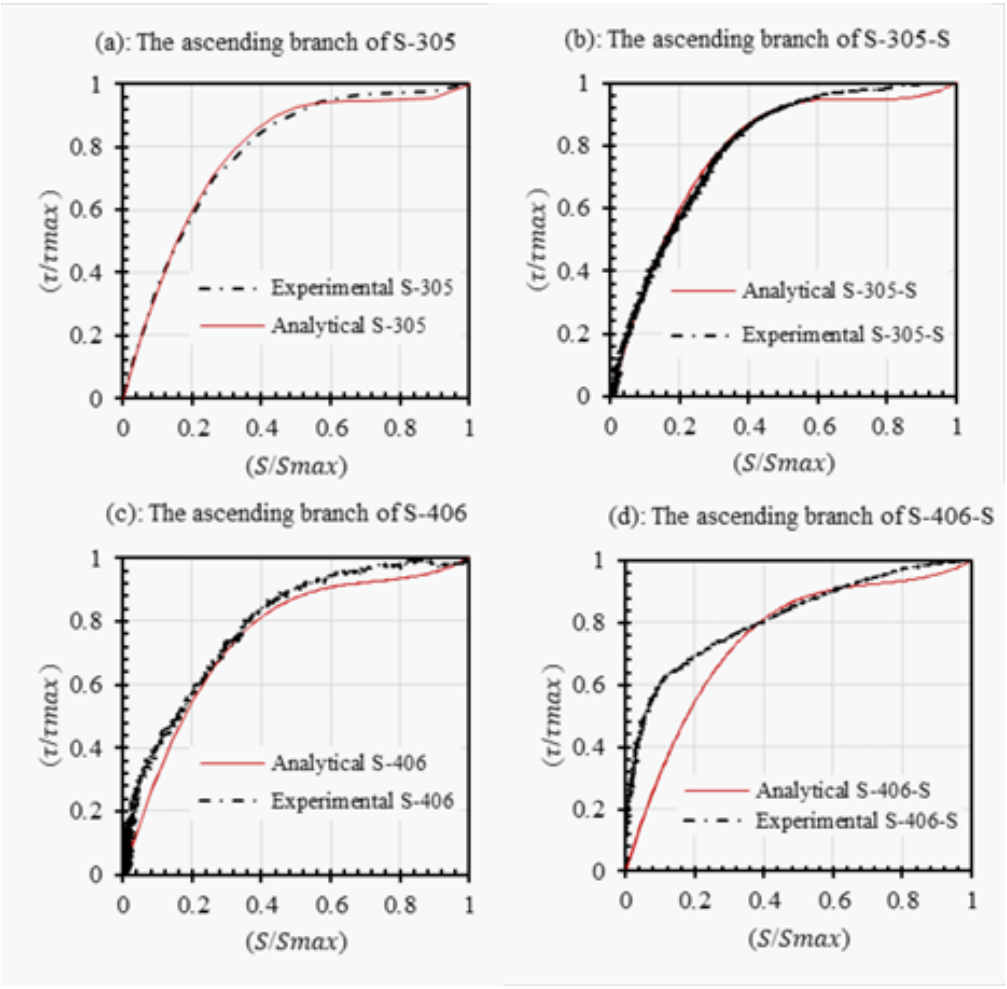

Figure 11: Comparison between the ascending branch of the analytical and experimental bond-slip model for CFFT members.

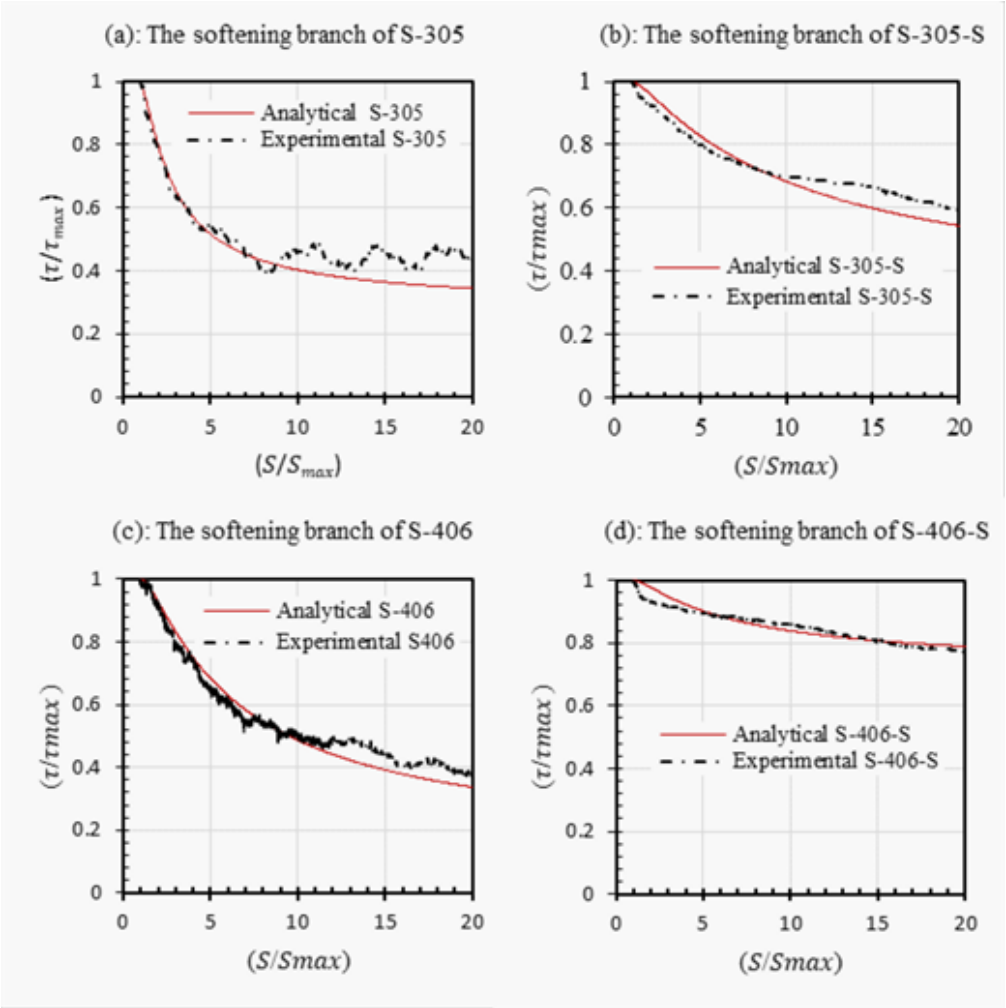

Figure 12: Comparison between the softening branch of the analytical and experimental bond-slip model for CFFT members.

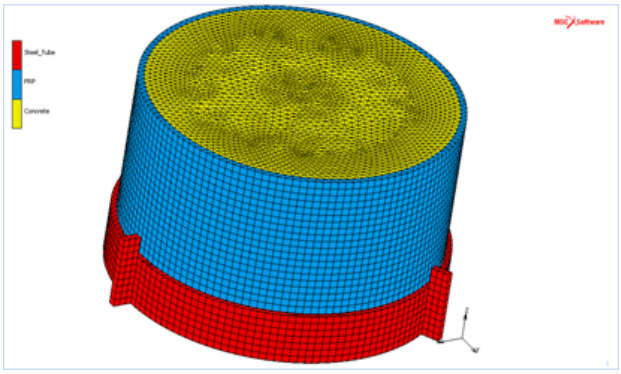

Figure 13: Finite Element Modeling : 3D Full Model

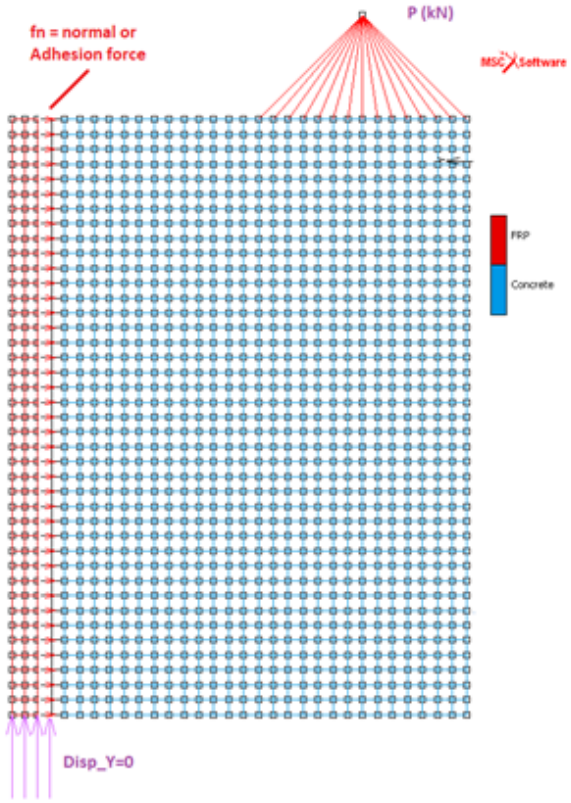

Figure 14: Finite Element Modeling : 3D - Axisymmetric model

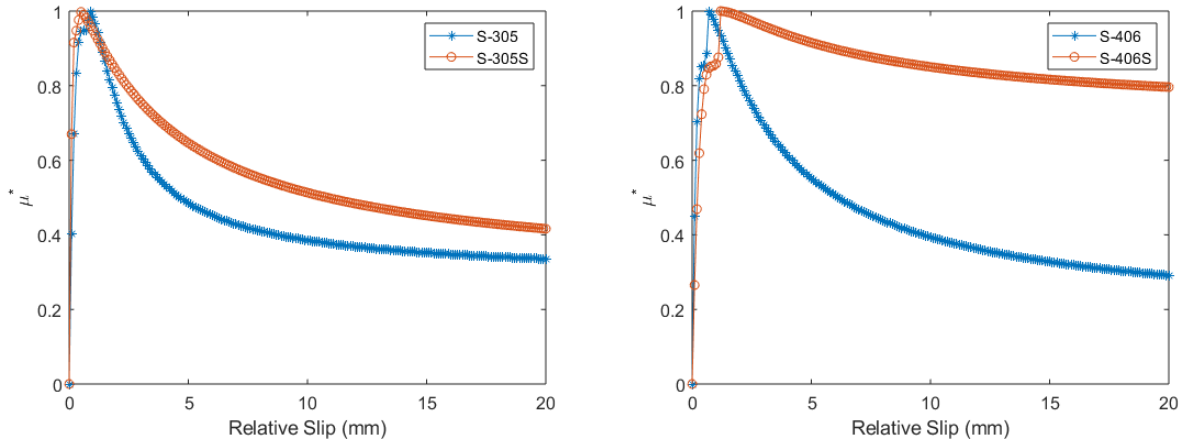

Figure 15: Evolution of the normalized friction coefficient identified from the experimental results and the analytical model

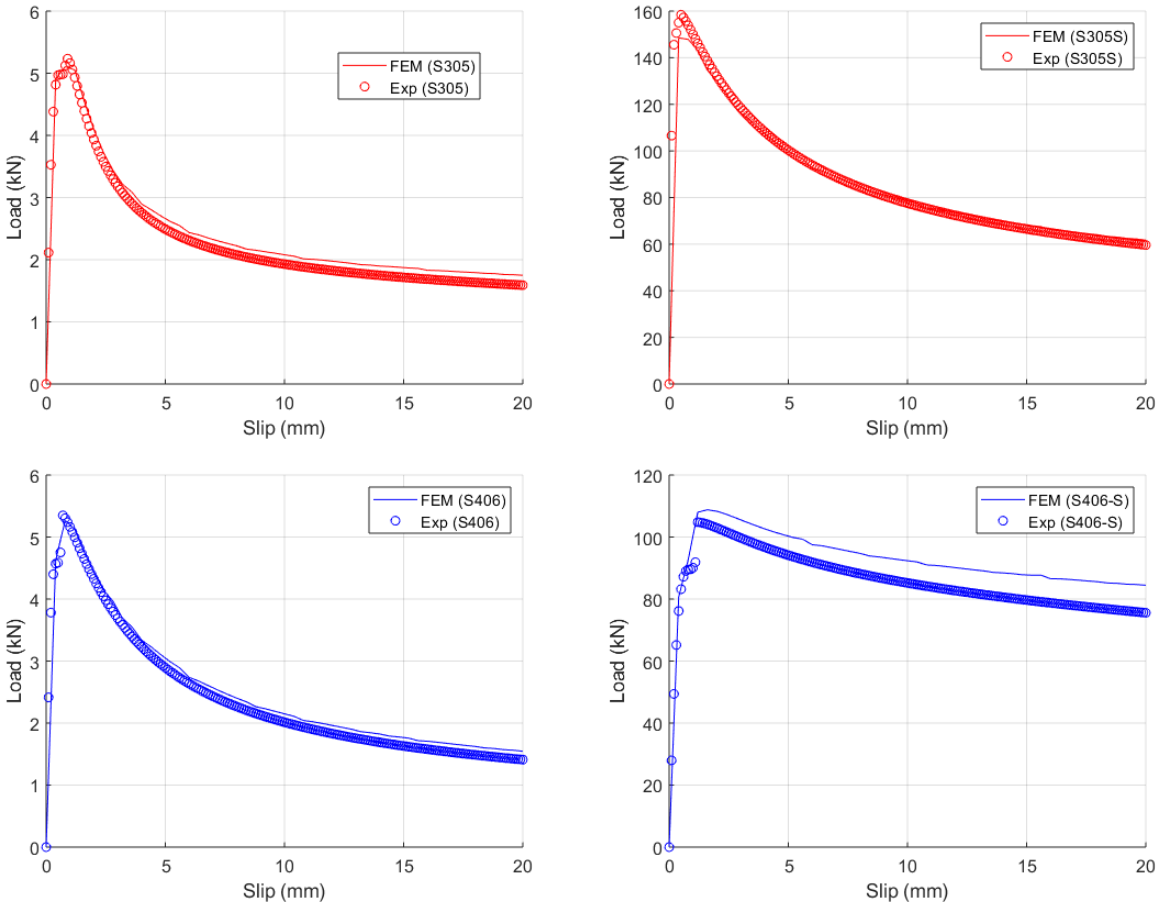

Figure 16: Comparison between the Finite element Model and experimental loads for CFFT members

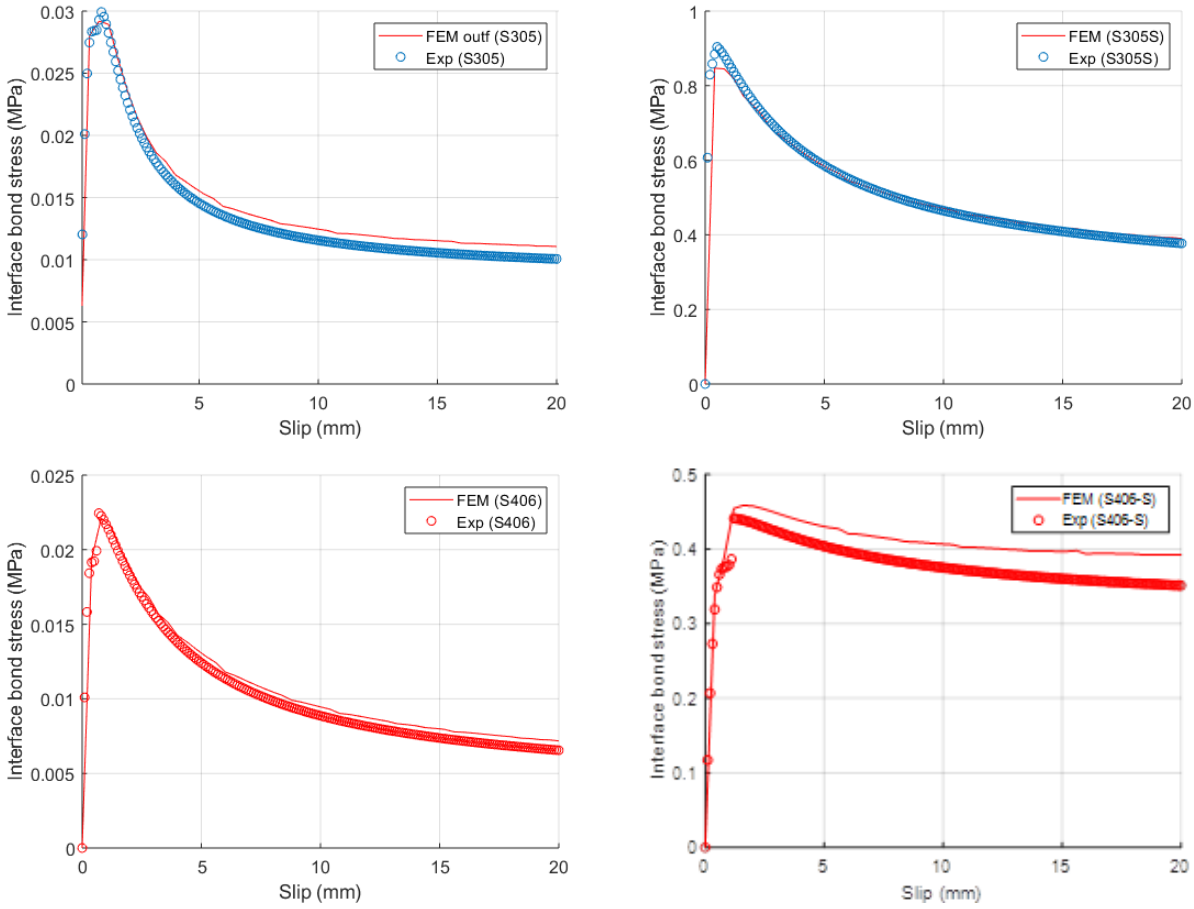

Figure 17: Comparison between the Finite element Model and experimental interface stresses for CFFT members

Highlights

- The interfacial bond between the pultruded FRP-Tubes and its Concrete Core ha experimentally investigated.
- The interfacial bond strength between the studied pultruded FRP-T and its CC can be neglected due to the smooth texture of the interior surface of the FRP-Tube.
- Using sand-coating as a bond enhancer improved the interfacial bond of the CFFT member by 2000% to 3000% in comparison to the specimens without sand-coating.
- An analytical bond-slip model for CFFT member is proposed based on the experimental results.

Declaration of interests

☒ The authors declare that they have no known competing financial interests or personal relationships that could have appeared to influence the work reported in this paper.

☒The authors declare the following financial interests/personal relationships which may be considered as potential competing interests: